Universal Behaviour in Erosive Burning of Solid Propellants

H. S. MUKUNDA* AND P. J. PAUL

Department of Aerospace Engineering, Indian Institute of Science, Bangalore 560012, India

This paper considers the extensive data and correlations on the erosive burning of solid propellants. A relatively simple nondimensional relationship between the ratio of the actual to nonerosive burn rate (η) and a quantity g, which is the product of g_0—the ratio of free stream mass flux to the mass flux from the surface for nonerosive condition—and Re_0^m, where Re_0 is the Reynolds number based on the nonerosive mass flux of the propellant and port diameter, is shown to correlate most data within the accuracies of the experiments with $m = -0.125$. This shows the above relationship to account for the effects of pressure, aluminum, even up to a proportion of 17%, burn rate catalysts, and motor size. It is concluded that the suggested correlation between η and g may be adopted universally for most practical propellants. © 1997 by The Combustion Institute

NOMENCLATURE

a	burning rate constant
AP	ammonium perchlorate
B	transfer number in Eq. 7
c_f	skin friction coefficient
c_{f_0}	skin friction coefficient at zero blowing
CMDB	composite-modified double base
c_p	specific heat of gases at constant pressure (J/kg K)
c_s	specific heat of solid propellant (J/kg K)
d_0	initial port diameter
DEP	diethylphthalate
G	mass flux through the port (kg/m^2 s)
g_0	ratio of port mass flux to nonerosive propellant mass burn rate ($G/\rho_p r_0$)
g	$g_0(\mathrm{Re}_0/1000)^{-0.125}$
g_{th}	threshold value of g
HMX	cyclotetramethylene tetranitramine
$\mathscr{H}(\ )$	heaviside step function
K_1	constant in Eq. 10
m	exponent in Eq. 9
n	exponent in Eq. 7
NC	nitrocellulose
NG	nitroglycerine
p	pressure
r	propellant burn rate
Re_0	Reynolds number based on propellant burn rate ($\rho_p r_0 d_0/\mu$)
r_0	burn rate at zero cross-flow velocity
RDX	cyclotrimethylene trinitramine
T_f	flame temperature
T_s	surface temperature
T_{in}	initial temperature of the propellant
α	constant defined by Eq. 2
α'	constant in Eq. 5
β	constant in Eq. 1
ρ_p	density of the propellant
η	ratio of erosive to nonerosive burn rate
τ	$(T_f - T_s)/(T_s - T_{\mathrm{in}})$

1. INTRODUCTION

Extensive experimental and modeling studies on both double-base and composite propellants have been reported and a summary of these studies was presented by Razdan and Kuo [1]. This comprehensive review presents a view of the influences of propellant composition, pressure, and initial temperature on the erosive burning characteristics. The discussion provides physical explanations of several of the effects and presents more than 25 correlations from different authors. Most of the correlations are based on fluid dynamic effects and are presented in dimensional form with parameters like total burn rate, the erosive component of the burn rate, pressure, mass flux, and the geometric dimensions appearing explicitly. Even those correlations which can be condensed into nondimensional form have not been so treated and several of the later correlations cannot be condensed into nondimensional form without involving dimensional unknown constants. In 1985, King [2] presented a

*Corresponding author.

0010-2180/97/$17.00
PII S0010-2180(96)00150-2

correlation of his own data, based on the velocities of the transverse flow and flame temperature of the propellant. One of the early studies in the modeling of erosive burning is that of Lenoir and Robillard [3]. Although this work, which laid the foundation for describing the erosive burning effects, has been adequately recognised, with few exceptions [4–7] later workers who have attempted to correlate their data have not benefited from this simple and elegant correlation. The original format of the correlation of Lenoir and Robillard [3] in dimensional form is

$$r = ap^n + \frac{\alpha G^{0.8}}{L^{0.2}} \exp\left(\frac{-\beta \rho_p r}{G}\right), \tag{1}$$

where L is the characteristic length argued to be the axial distance in the original work [3], but modified to be the port diameter by some later workers [5, 6] G is the mass flux, and β is a dimensionless constant. The constant α depends on the density of the propellant ρ_p, the flame and surface temperature T_f and T_s, the gas phase viscosity μ, and the specific heats in the condensed and gas phases c_p and c_s. Its functional form is

$$\alpha = \frac{0.0288 c_p \mu^{0.2} \Pr^{-2/3}}{\rho_p c_s} \frac{(T_f - T_s)}{(T_s - T_{\text{in}})}, \tag{2}$$

where T_{in} is the initial temperature of the propellant. Equation 1 can be recast by recognising the nonerosive burn rate, r_0 as $r_0 = ap^n$ and defining η as r/r_0 and $g_0 = G/\rho_p r_0$, to give

$$\eta = 1 + 0.0288 \frac{c_p}{c_s} \mathrm{Re}_0^{-0.2} \Pr^{-2/3} \tau_f g_0^{0.8} \times \exp\left(\frac{-\beta \eta}{g_0}\right), \tag{3}$$

where Re_0 is a Reynolds number defined by $\mathrm{Re}_0 = \rho_p r_0 L/\mu_0$ and $\tau_f = (T_f - T_s)/(T_s - T_{\text{in}})$. The ratio of the gas phase to condensed phase specific heats is about 1, and τ_f can be estimated from the data on flame and surface temperatures for low- to high-energy propellants to be between 1.3 and 4.0. One can postulate the functional relationship in erosive burning as

$$\eta = \eta(g_0, \mathrm{Re}_0, \tau_f, r_r), \tag{4}$$

where r_r is the roughness normalised by the local boundary layer thickness, which is expected to influence the burn rate [7–10]. In Eq. (4), the primary influence on η comes from g_0. Equation 3 can be finally written as

$$\eta = 1 + \alpha' g_0^{0.8} \exp(-\beta \eta / g_0), \tag{5}$$

where α' is composed of the various quantities in Eq. 3. In order to account for roughness, it is more appropriate to start with a relationship like

$$\eta = f(c_f, g_0), \tag{6}$$

where c_f is the skin friction coefficient which is a function of blowing (actual burning rate) and roughness. It can be written as

$$c_f = c_{f0} B^{-n}, \tag{7}$$

where $B = \rho_p r / G c_f$ is the transfer number and n has a typical value of 0.77 [11]. Modifications to this expression because of differences in densities between the surface and the free stream due to the molecular mass of gases and temperature were provided by Paul et al. [12]. These expressions are complex and cannot be used here directly. The principal point of the work of Paul et al. [12] is that the exponent is close to 0.5. In this work we only use the functional relationship. One then obtains

$$c_f = c_{f0}^{1/(1-n)} (g_0/\eta)^{n/(1-n)}. \tag{8}$$

Furthermore, c_{f0} is a function of axial Reynolds number $G d_0/\mu$ and roughness r_r. This dependence was described for flow over a flat plate by Sclichting [13]. If one were to describe the dependence of c_{f0} on Re_0 in a form $c_{f0} \sim \mathrm{Re}_0^l$, then l has a value of 0.2 in the smooth flat plate case. With roughness, l varies between -0.2 to $+0.2$ depending on the value of axial Reynolds number and roughness. We can combine the above arguments and from Eqs. 6 and 8, we can write

$$\eta = f(g_0 \mathrm{Re}_0^m). \tag{9}$$

In the present case, there is also the effect of blowing. The combined effects can be set out in terms of a constant exponent on Re_0 for simplicity. Following the classical understanding of the presence of threshold mass flux [1], we can write the erosive burning relationship as

$$\eta = 1 + K_1(g^{0.8} - g_{\mathrm{th}}^{0.8})\mathscr{H}(g - g_{\mathrm{th}}) \tag{10}$$

with

$$g = K_2 g_0 \,\mathrm{Re}_0^m, \tag{11}$$

where $\mathscr{H}$ is the Heaviside unit step function. The values of K_1 and g_{th} are determined from actual data. Any convenient value can be chosen for K_2, as it only affects the scaling. (Equation 11 substituted into Eq. 10 gives a single constant $K_1 K_2^{0.8}$. For any arbitrary value of K_2, K_1 can be obtained by keeping $K_1 K_2^{0.8}$ constant. A second constant is used only as a scaling factor for g, so that the range of magnitudes of g and g_0 are the same.) The Reynolds number Re_0 is based on the nonerosive mass burn rate and the port diameter. It must be remembered that the primary effect is expressed through the term $g^{0.8}$, which accounts for the mass flow effect and the Reynolds number correction is to account for the size effect.

2. HYPOTHESIS

It is hypothesized that the all effects of erosive burning are contained in a unique relationship between η and g. The effects of other parameters are considered subsidary. This hypothesis was tested in a limited sense (without the Re_0 effect) in an earlier work [7] and found reasonable for data from many sources. Subsequent to this work, some valuable data by Ishihara and Kubota [14] came to light and it was therefore thought worthwhile to revisit the issues raised by the hypothesis. In order to help assess these data, most available experimental data are identified in Table 1. This table contains the source of the data, the propellants for which the data are obtained, the density, the flame temperature of these propellants, and the characteristic dimension (L) of the system used in the tests. Except for the case of Marklund and Lake [15], the hydraulic diameter of the port is taken for L. In the case of Marklund and Lake the effective dimension is taken to be the size of the tablets used in the experiments. After some numerical experiments, the value of m was chosen as -0.125 to reduce the error in the curve fit. This implies an expression for g of $g = g_0(\mathrm{Re}_0/1000)^{-0.125}$. This also gives the size dependence of $d^{-0.1}$ indicated by Nagaoka et al. [6]. The value of K_2 in Eq. 11 is arbitrarily chosen as $1000^{0.125}$ to reduce the variation in the magnitude of g, since in most applications the value of Re_0 is in the range of thousands.

A few comments about the hypothesis are in order. A study of most earlier work including the review article by Razdan and Kuo [1] leads to an understanding that erosive burning is a complex function dependent on a large number of parameters which include port mass flux, pressure, composition with metal content explicitly considered, nature of binder, oxidiser particle size in the case of composite propellants, and geometry of the port of the motor. The importance of fluid mechanics for erosive burning is brought out, but no explicit attempt has been made to separate this effect and seek the subsidiary influences. The primary attempt here is to capture the major influence through the choice of the parameters which encompass several aerothermal effects and to examine whether the data show distinct trends beyond these effects. By choosing r_0 in the denominator of the expression for g_0, the influence of oxidiser particle size, pressure, and composition are taken into account. Furthermore, the port geometry effects are essentially gas dynamic—changing the local static pressure and thus influencing r_0—apart from influencing the local lateral mass flux, which again is accounted for in the numerator of the expression for g_0. It may be argued that if the propellant composition is highly fuel rich, as may happen in low-energy propellants, it will show distinct chemical kinetic influence beyond the fluid mechanical effects caused by g_0. These can be understood only after plotting the experimental data in the above-mentioned coordinates.

TABLE 1

Propellants for which Erosive Burning Data are Available

Code	Propellant Composition	ρ_p (kg/m^3)	T_{ad} (K)	d_0 (mm)
Ishihara and Kubota [14]				
High energy	55.6NC + 40.4NG + 4.0DEP	1600	2716	20.0
Reference	50.4NC + 36.6NG + 13.0DEP	1600	2114	
Low energy	47.5NC + 34.5NG + 18.0DEP	1600	1778	
Marklund and Lake [15]				
Prop A	65AP (24–30 μm) + 35polyester	1620	1690	5.0
Prop C	75AP (24–30 μm) + 25polysulfide	1700	2550	
Lawrence et al. [5]				
Prop 1	68AP + 16Al + 16UTREZ	1700	—	12.5
Prop 2	84AP + 16UTREZ	1700	—	
Prop 3	68AP + 16Al + 16(PBAN + Fe_2O_3)	1700	—	
Prop 4	68AP + 16Al + 16PBAN	1700	—	
Prop 5	72AP + 14Al + 16(CTPB + Fe_c2O_3)	1720	—	
Prop 6	73AP + 10Al + 17CTPB	1680	—	
Nagaoka et al. [6]				
	65AP + 16Al + 19PB	1550	—	20–90
King [25]				
4525	73AP (20 μm) + 27HTPB	1500	1667	19
5051	73AP (200 μm) + 27HTPB	1500	1667	
4685	73AP (5 μm) + 27HTPB	1500	1667	
4869	72AP (20 μm) + 25HTPB + $2Fe_2O_3$	1500	1660	
5542	77AP (20 μm) + 27HTPB	1550	2065	
5565	68.4 (200 μm) + 13.6 (90 μm) AP + 18HTPB	1650	2575	
5555	41 (1 μm) + 41 (7 μm) AP + 18 HTPB	1650	2575	
6626	70 (90 μm) + 4 (200 μm) AP + 21 HTPB + 5Al	1600	2575	
Razdan and Kuo [9]				
4525	73AP (20 μm) + 27HTPB	1500	1667	15
5051	73AP (200 μm) + 27HTPB	1500	1667	
	76AP (76 μm) + 24(PBAA + EPON)	1500	1920	
Godon et al. [17]				
	80AP + 20CTPB	1590	2313	3–5
Strand et al. [24]				
	70AP + 14PBAN + 16Al	1770	3200	52, 102
Traineau and Keuntzmann [18]				
	70AP + 14PBAN + 16Al	1770	3200	20
Osborn et al. [19]				
	65AP + 18CTPB + 17Al	1790	3100	

3. DISCUSSION OF THE EROSIVE BURNING DATA

3.1. Data of Ishihara and Kubota

As can be noted from Table 1, the experimental data of Ishihara and Kubota [14] are for three double-base propellants, one of which is termed reference and two others that have higher and lower energy than the reference propellant. The degree of fuel richness also varies among the three propellants. The variation in energy is obtained by changing the relative proportion of NC/NG/DEP. The nonerosive burn rate varies by a factor of more than 2. The experiments were limited to one pressure (2 MPa). Figure 1 shows the original data on η vs cross-flow velocity as given by Ishihara and Kubota [14] and η vs g as conceived here. The scatter in the original data increases to about 10% at high velocities. The data condense into a single plot in the η vs g format. The total number of data points presented here is 66. The threshold velocities for the three cases are 60, 80, and 200 m/s for low-energy, reference, and high-energy propellants, respectively. The threshold g, denoted

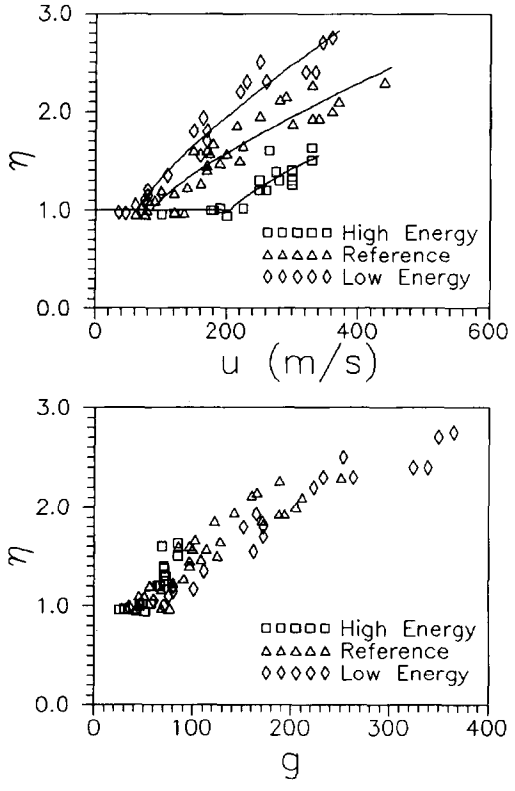

Fig. 1. Data of Ishihara and Kubota [14] (a) in terms of η vs u (m/s) and (b) in terms of η vs g (present work).

by g_{th}, is in the range 40–50 from Fig. 1 when all the data are taken together. Thus the double-base propellants, with a reasonably large range of nonerosive burning rates and energy, seem to follow the η vs g relationship quite well. The data for the three cases merge within the scatter, implying there is no effect other than fluid mechanical in these results.

3.2. Data of Marklund and Lake

The data of Marklund and Lake [15] have been used by researchers [16, 7] to compare the model predictions. The results are on buttons of propellants and are reportedly quite accurate ($\sim$ 3–5%). The original data and the data on the η vs g plot are presented in Fig. 2. It can be seen clearly that the data condense quite well on the nondimensional coordinates. A further point about this plot is that the results at various pressures still fall on the same curve. Thus the effect of pressure, apart from what comes through the nonerosive burn rate (which is taken into account in the normalisation), is essentially fluid mechanical, namely, an increase in mass flux through an increase in density. The total number of data points here is 29. The critical flux g_{th} in this case is about 35. Furthermore, even though the results are on two binders, namely, polyester and polysulfide, there are no effects special to the binder.

The marginal crossover of the results for cross-flow velocity of 54 m/s for propellant C with nonerosive burn rates has been thought to be due to possible negative erosion. A careful examination of the data shows that the differences are about 3%. This is within the stated accuracies of experiments. The experimental data can be looked upon as revealing a threshold flux corresponding to cross-flow velocity of 54 m/s.

3.3. Data of Lawrence et al.

The data of Lawrence et al. [5] are on high-energy propellants. They have high solid loading and most of them are aluminised to the same extent as in practical systems. The authors used the correlation owing to Lenoir and Robillard [3], which was discussed earlier, by taking the parameter α as a constant for all the propellants based on the argument that the combustion properties were similar. However, the density of the propellant and flame and surface temperatures will be different for aluminised and nonaluminised propellants. The value of the constant α' will depend on the density of the propellant, the nonerosive burn rate, and the characteristic dimension D or L. Based on the suggestions of these authors as well as Nagaoka et al. [6], the use of the port diameter, d_0 for L has been made here. Even though Lenoir and Robillard suggested a value for β of 53, Lawrence et al. [5] used a value of α' given by thermochemical parameters and different values of β for different propellants to fit the pressure–time data. These are shown in Table 2. A solution of the implicit transcendental equation (Eq. 5) for the chosen parameters in Table 2 gives η vs g. This relationship is presented in Fig. 3. As can be seen, with the exception of one propellant, most data fall into a narrow band, even though the density, ener-

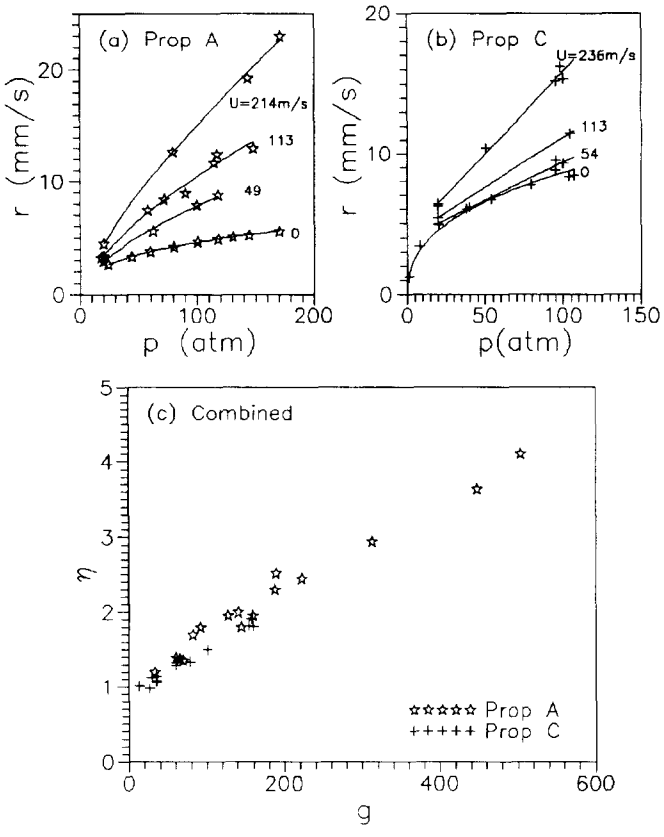

Fig. 2. Data of Marklund and Lake [15] (a, b) in terms of burn rate (r) vs p and velocity and (c) in terms of η vs g.

getics, and composition are widely different. The data of the propellant 5 are below those of others (the reasons for this cannot be unravelled with the available information in the paper by Lawrence et al.), but within the larger band of uncertainties of erosive burning data.

From their experiments, Nagaoka et al. [6] obtained the parameters in Lenoir and Robillard's relationship and when they were nondimensionalised they gave $\alpha' = 0.027$ and $\beta = 80$. These fall within the data band of Lawrence et al. presented in Table 2. Nagaoka et al. indicated that this correlation is not very satisfactory when scaled up for large motors, and they provided another correlation with critical mass flux as the parameter. The critical mass

TABLE 2

Parameters for the Experimental Data of Lawrence et al. [5]

Propellant Composition	α'	β
68AP + 16Al + 16UTREZ	0.026	60
84AP + 16UTREZ	0.026	65
68AP + 16Al + 16(PBAN + Fe_2O_3)	0.026	70
68AP + 16Al + 16PBAN	0.026	60
72AP + 14Al + 16(CTPB + Fe_2O_3)	0.028	125
73AP + 10Al + 17CTPB	0.028	85

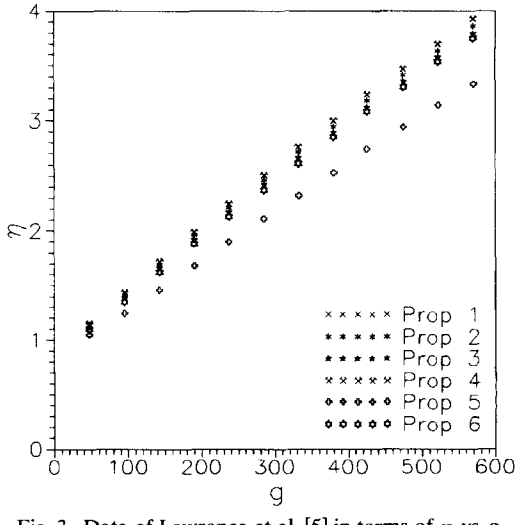

Fig. 3. Data of Lawrence et al. [5] in terms of η vs g.

flux given for two specific experiments gives $g_{th} = 35$ and 37.

3.4. Results of Godon et al., Traineau and Kuentzman, and Osborn et al.

Godon et al. [17] reported experimental results on composite propellants (80% AP/20% CTPB) with a basic burn rate varying from 9.9 to 26.3 mm/s. The burn rate variation was achieved with the addition of a catalyst to the basic propellant formulation. Traineau and Kuentzman [18] presented the data of η as function of mean cross-flow velocity with initial velocity and nonerosive burn rate as parameters, while Osborn et al. [19] plotted burn rate against pressure at various cross-flow velocities. All these data are plotted in the present coordinate system in Fig. 4. They fall into a small band, as can be seen from the figure.

Figure 5 contains all the data discussed above, of which three are for double-base and the others are for state-of-the-art high-energy propellants. Most of the data are within $\pm 10\%$. They cover a wide range of practical applications in terms of cross-flow velocities and pressures. These authors made another important observation: that pressure has no significant effect on the erosive burning parameters. This is quite consistent with the results of Marklund and Lake, which are presented in Fig. 2.

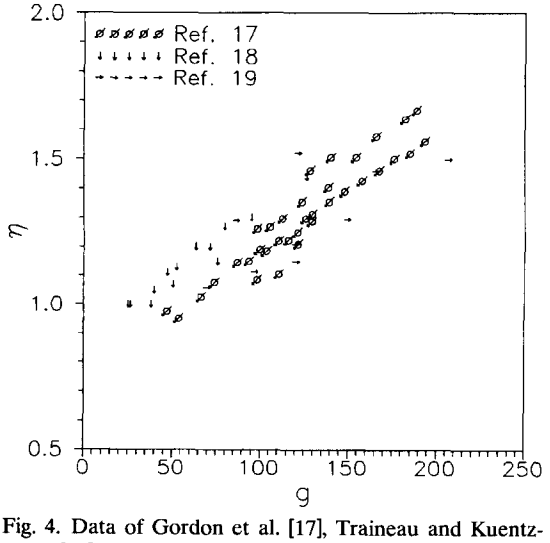

Fig. 4. Data of Gordon et al. [17], Traineau and Kuentzmann [18], and Osborn et al. [19] in terms of η vs g.

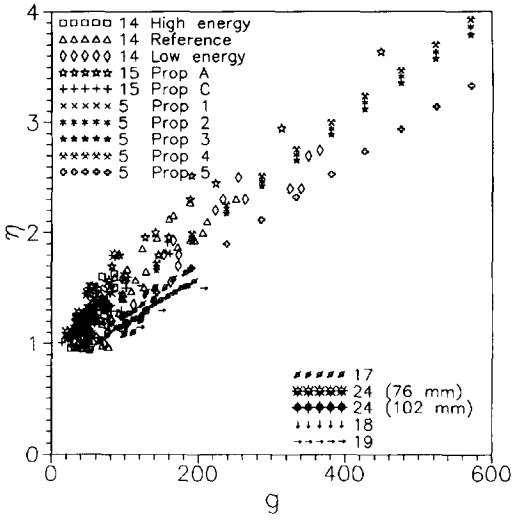

Fig. 5. Comparison of data from Ishihara and Kubota [14], Marklund and Lake [15], Lawrence et al. [5], Godon et al. [17], Traineau and Kuentzmann [18], and Osborn et al. [19] on η vs g plot. The legend indicates reference number and propellant identification.

3.5. Results of Strand and Cohen

Strand, Cohen, and others [20–24] experimented on two different motor sizes to examine the size effect on the erosive augmentation of burn rate. They used two different motor sizes, of diameters 305 and 127 mm, with grain port diameters of 102, 153, and 52 mm, respectively. A careful analysis of the data shows that for a large size motor with 102 mm i.d. grain there are anomalies in the data which have been attributed to the data processing methods and electrical noise in the web measurement system [21]. In the experiments with 153 mm i.d. grain the extent of erosive burning is very small. The authors have tried to explore the possibility of correlating the data using several independent parameters—Reynolds numbers based on axial mass flux, as well as surface transpiration Reynolds number (Re_0 in this paper), $G^{0.8}$, and variants of these combined with threshold values (which need to be assessed independently). Based on the study, it is concluded that there is a size effect, beyond the classical boundary layer analysis. Many of these correlations suggest a diameter effect in dimensional terms. However, one of these correlations, namely, η vs G/G_{th}, shows no size effect. All these correlations are different from

the present ones. Nevertheless, the issue of size dependence being different was tested within the framework of the current study by choosing the exponent on the Re_0, m of Eq. 11, to be -0.4. This study showed the correlation with an exponent of 0.125 to be distinctly superior to one of 0.4 as shown in Fig. 6. Furthermore, Nagaoka et al. [6] conducted experiments on different size motors and concluded that erosive burning has a size effect given approximately by $d^{-0.1}$ and they confirmed the results in motors of diameter up to 1400 mm.

3.6 Results of King and Razdan and Kuo

King [25] presented experimental results on the erosive burning data for several composite propellants designed primarily to extract the effects of propellant composition variables, like AP particle size, burn rate modifiers, and aluminum fraction. Subsequently, the same data were presented in another paper in 1981 [26] along with error estimates for mass flux and nonerosive burn rate to enable estimates to be made of augmentation in burn rate. Of the eight propellants studied by King [25], Razdan and Kuo [10] studied two experimentally. The nonerosive burn rate data of these two propellants (designated 4525 and 5051) from the two sources [26, 10] are different by about 5% at operating pressures (3.0–7.2 MPa). The comparison between the two sources made by Razdan and Kuo [10] of the erosive component of the burn rate with pressure at various velocities shows significant differences for the same propellant. This is argued to be possibly due to the data reduction procedure adopted by King. The accuracy is stated to be improved through repeated reading of films to measure the web thickness with an accurate motion analyzer. However, these differences are not mitigated by the additional difference of 5% in the nonerosive burn rate between the two studies. In summary, the results of these authors have significant differences, typically amounting to ± 10–15%, with an error that is higher at larger velocities and mass flux. Two typical plots in terms of η vs g for propellants 4245 and 5051 are shown in Fig. 7. While for propellant 4525, though the scatter in the data is high, the data trends seem preserved, in the case of propellant 5051, even the trends seem to be at variance. The data of King seem closer to most other data discussed earlier, whereas those of Razdan and Kuo show a much stronger dependence of η on g. King's data for all the propellants from his work are presented in Fig. 8. It can be seen that scatter in the data increases with g increasing up to $\pm 15\%$ at large g. Perhaps better accuracies cannot be expected in these difficult experiments. The total number of data points is 140 for pressures from 1 to 10 MPa. Despite the two propellants

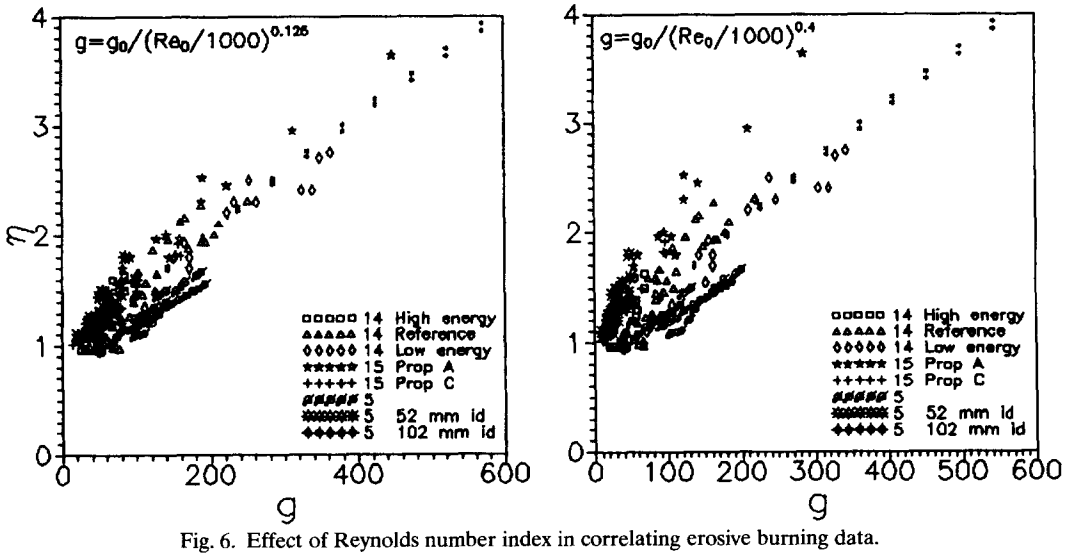

Fig. 6. Effect of Reynolds number index in correlating erosive burning data.

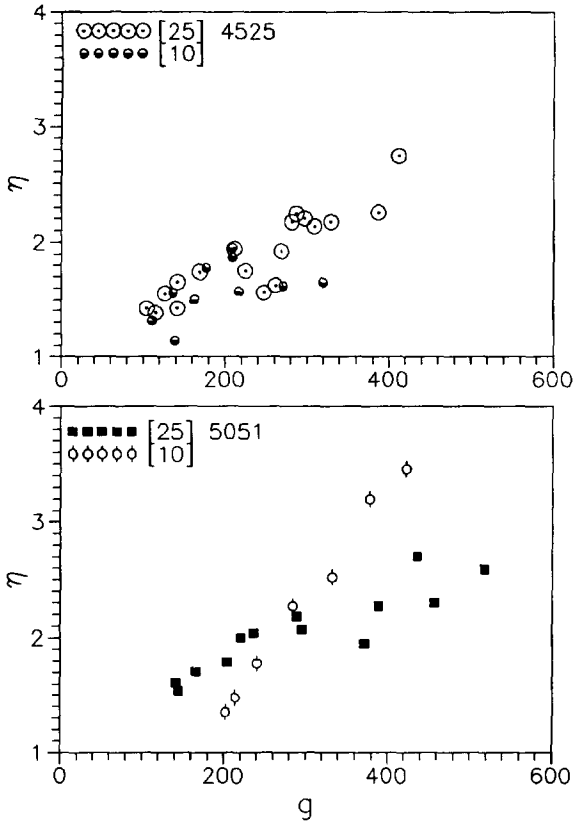

Fig. 7. Comparison of data from King [25, 26] and Razdan and Kuo [10] for propellants 4525 (a) and 5051 (b). The legend indicates reference number and propellant identification.

4685 and 5542 showing some departures, it appears that most of the data show a single trend of η vs g within the scatter of the data of individual propellants (for instance, propellant 4869 shows close to 15% scatter around its mean), irrespective of the particle size of AP or the extent of loading, presence or absence of catalysts, and pressure.

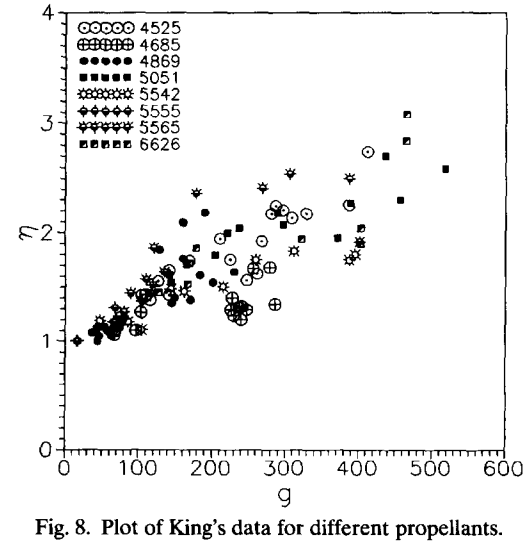

Fig. 8. Plot of King's data for different propellants.

3.7. Motor Geometry and Size Effects

The motor geometry exerts a strong influence on the role of erosive burning in actual motors. A careful study of Williams et al. [27] and Razdan and Kuo [1] shows that cause and effect of the motor geometry are not clearly established. It is yet to be recognised that the negative erosion effects in the star grain configurations could be due to nonuniform flow field, with the relevant mass flux affecting the burn rate in the star point region different from the mean. The discussion on the nonuniform port geometry [1, p. 586] presents gas dynamic changes which can legitimately affect the local burn rates along with the axial divergence affecting the deceleration and thickening of the boundary layer in such a manner that the two effects are not isolated. The question arises whether there are effects caused by

boundary layer related features, beyond the known grain geometric related effects. Such effects, if dramatic, should have appeared in the results of Lawrence et al. [5] since they used motor data to extract the erosion constants. Hence, it appears to us that erosion effects beyond those of the above expression for erosive burning enhancement are within the noise of the experimental data. To this end, the data of Razdan and Kuo [28] were analysed. They showed most of the motor size effect to be essentially gas dynamic related, and the true size effect to be about 8%. This is accounted by the Re_0 term in the above relationship. The curve-fitted plot of enhanced erosion with port diameter at fixed velocities leads to $(\eta - 1) \sim d_0^{-0.11}$, which confirms the Reynolds number dependence in the present relationship. Nagaoka et al. [6] expressed concern regarding the overprediction of erosive burning effects by the Lenoir and Robillard relationship in large size motors when the parameters in the relationship were derived from small sized motors. They suggested a relationship based on mass fluxes with a correction factor of $d_0^{-0.1}$. This is consistent with the present expression in which the exponent of -0.125 on Re_0 was obtained by minimising the error in the curve fit of small motor data.

3.8 All the Data

Figure 9 is a plot composed of all data discussed above. It also contains a few data points from the work of Green [29], whose data have also been analysed by Miller [4]. The total number of data points covered is 390 (discrete). The data of the work of Lawrence et al. [5] and Nagaoka et al. [6] are to be counted in addition. They have provided the parameters in a law, and since it is difficult to assess the actual number of data points contributed by these data, they are taken to be 60 data points with 10 for each data set. The mean and $\pm 15\%$ line are drawn through the data points. The total number of data points covered within this band is 373 and outside 77. These are interpreted to mean that a single curve fit gives the erosive burning correlation for all the propellants, particularly the high-energy state-of-the-art composite (C), double-base (DB) propellants. It is

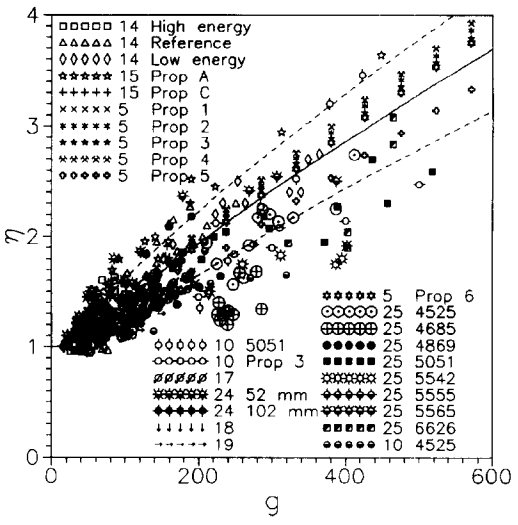

Fig. 9. Plot of η vs g for data of all authors for both double-base and composite propellants.

conjectured that composite-modified double-base propellants (CMDB) will also follow similar trends since HMX-, or RDX-based CMDB propellants have been shown to be similar to DB propellants [30] and fluid mechanical effects will not distinguish between these propellants. Somewhat similar arguments can be made for AP-based CMDB propellants since the modification due to AP will be to enhance the diffusional contribution to the burning structure of the basic propellant. The fact that the data from a wide range of compositions and flow conditions follow a trend on this plot implies that there is a universality in the erosive burning behaviour. This arises from the dominant control of fluid dynamics. The mean line through all the data leads to the equation $\eta = 1 + 0.018(g^{0.8} - g_{th}^{0.8})\mathscr{H}(g - g_{th})$, where $g_{th} = 35$.

3.9 Validation by Prediction of Pressure–Time Trace

The prediction of pressure–time curve using the proposed correlation has been attempted for the motors of Nagaoka et al. [6]. Nagaoka et al. gave the head end pressure versus time data for motors of diameters ranging from 30 to 135 mm and grain initial port diameters from 20 to 90 mm, respectively. The grain lengths and throat diameters have been chosen

such that the initial K_i (ratio of burning area to port area) and K_n (ratio of burning area to nozzle throat area) remain the same in different size motors, so that the nonerosive pressure–time traces on a scaled time coordinate are identical in different size motors. Experimental results for 20 and 90 mm port diameters are shown in Fig. 10. An important feature of the data is that the differences in pressure versus time plot are only due to the size effect on erosive burning because the initial K_i and K_n are held constant, and the size effect is distinctively exposed. Predictions of the pressure versus time data have been made by numerically solving one-dimensional time dependent conservation equations of mass, momentum, and energy in the grain port [31]. The comparison for 20 and 90 mm port grains is also shown in Fig. 10.

In order to obtain a good match with the observed pressure–time trace, it was necessary to increase the constant of Eq. 10 from 0.018 to 0.023. Although the curve with an increased constant would still be within the scatter of the data, it lies toward the upper bound. Numerical experiments with different exponents on Re_0 have shown -0.125 to be the best value. Finally, to ascertain if 0.023 is a reasonable choice of the constant K_1, a plot of the data from the experiments discussed earlier, which have the least internal scatter, has been plotted along with the curve of Eq. 10 with $K_1 = 0.023$ in Fig. 11, along with the $\pm 10\%$ band. For these data the expression is a good fit. Considering these facts the universal expression for erosive burning is recommended as

$$\eta = 1 + 0.023(g^{0.8} - g_{\mathrm{th}}^{0.8})\mathscr{H}(g - g_{\mathrm{th}}), \quad (12)$$

where $g = g_0(\mathrm{Re}_0/1000)^{-0.125}$ and $g_{\mathrm{th}} = 35.0$.

4. CONCLUDING REMARKS

This paper has considered all the erosive burning data of a range of propellants from double-base to composite, varying energy levels, and different base burn rates. A simple hypothesis is that these data show a universality in the relationship between the erosive burning rate ratio and a nondimensional mass flux and the Reynolds number, based on the nonerosive burn rate and port diameter, with the underlying assumption that the phenomenon is fluid dynamically controlled. An examination of the data shows that such a hypothesis is indeed valid to within the experimental accuracies in the measurement. The chemical kinetic factors, if any, have such a minor role that they do not make any distinct contribution to the effects of erosive burning beyond experimental noise. The data are curve-fitted into an expression (Eq. 12) which can be used for most practical propellants to within $\pm 10\%$ accuracy.

One issue left unaddressed is that of negative erosion, which has been discussed in the literature. The most prominent data quoted

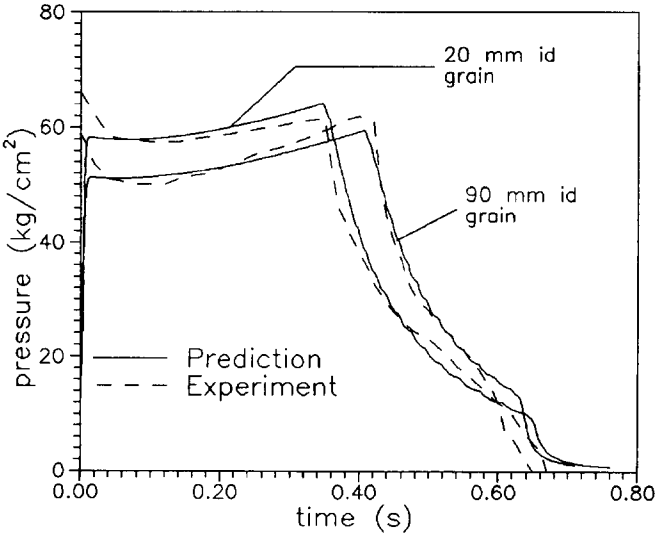

Fig. 10. Pressure–time traces of two motor sizes of Nagaoka et al. [6] and comparison with present predictions.

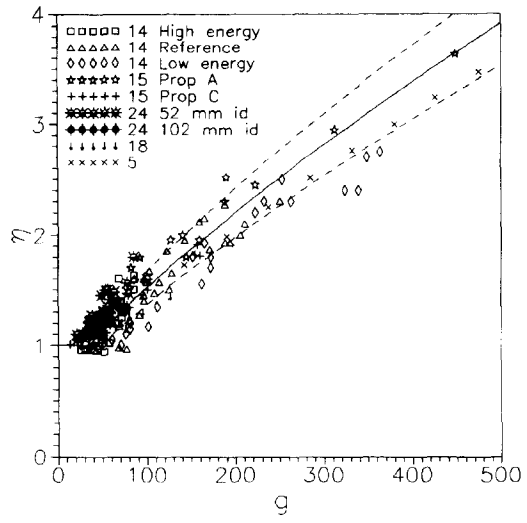

Fig. 11. Comparison of selected data with the recommended erosive burning law. Recommended fit and ±10% lines (dotted) are also shown.

are those of Zucrow et al. [32], which show substantial negative erosion. The full details of the experiment are unavailable to determine the causes for such effect. Two of the coauthors of this paper, while presenting the above work in a later paper, presented results from seemingly the same set of experiments which show results that exclude the set involving negative erosion [19]. Most of the other results which display negative erosion have deviations of η from unity so small that it is not obvious that they are significant (as in the case of Marklund and Lake [15] discussed earlier). While it may be possible that some propellants on binders like polyurethane display negative erosion, it must be pointed out that these propellants are of not-too-high a solid loading and therefore show larger binder thickness. This encourages melt layer to play a part in the burning mechanism. However, state-of-the-art propellants with high solid loading (87%) use binders such as PBAN, CTPB, and HTPB that do not show the phenomenon of negative erosion.

REFERENCES

1. Razdan, M. K., and Kuo, K. K. *Fundamentals of Solid Propellant Combustion.* AIAA, New York, (1983), chap. 10, pp. 515–597.
2. King, M. K., *AIAA J.* 22:394–395 (1985).
3. Lenoir, J. M., and Robillard, G., *Sixth Symposium (International) on Combustion*, The Combustion Institute, Pittsburgh, 1957, pp. 663–667.
4. Miller, E., *Combust. Flame* 10:330–336 (1966).
5. Lawrence, W. J., Matthews, D. R., and Deverall, L. I., *Third Solid Propulsion Propulsion Conference*, Atlantic City, NJ 1968, AIAA Paper No. 68-531.
6. Nagaoka, T., Shirota, K., Koreki, T., and Saito, S., *Tenth Space Science and Technology Symposium*, Tokyo, Japan, 1973, pp. 83–89.
7. Mukunda, H. S., *Combust. Sci. Technol.* 18:105–118 (1978).
8. Beddini, R. A., *AIAA J.* 16:898–905 (1978).
9. Razdan, M. K., and Kuo, K. K., *AIAA J.* 17:1225–1233 (1979).
10. Razdan, M. K., and Kuo, K. K., *AIAA J.* 18:669–677 (1980).
11. Marxman, G. A., and Gilbert, M., *Ninth Symposium (International) on Combustion*, The Combustion Institute, Pittsburgh, 1963, pp. 371–383.
12. Paul, P. J., Mukunda, H. S., and Jain, V. K., *Nineteenth Symposium (International) on Combustion*, The Combustion Institute, Pittsburgh, 1982, pp. 717–729.
13. Schlichting, H., *Boundary Layer Theory.* McGraw-Hill, New York, 1965.
14. Ishihara, A., and Kubota, N., *Twenty-First Symposium (International) on Combustion*, The Combustion Institute, Pittsburgh, 1986, pp. 1975–1981.
15. Marklund, T., and Lake, A., *ARS J.* 3:173–178 (1960).
16. Lengelle, G., *AIAA J.* 13:315–322 (1977).
17. Godon, J. C., Duterque, J., and Lengelle, G., *AIAA J.* 8:741–747 (1992).
18. Traineau, J., and Kuentzmann, P., *J. Propulsion and Power* 2:215–222 (1986).
19. Osborn, J. R., Rene, J. P., and Murphy, J. M., *Acta Astronautica* 11:459–467 (1984).
20. Strand, L. D., Yang, L., Ray, R., and Barry, J., *Twenty-Second JANAF Combustion Meeting*, 1985, CPIA Publication No. 432.
21. Strand, L. D., Yang, L., and Nguyen, M. H., *Twenty-Second Joint Propulsion Conference*, 1986. AIAA Paper No. 86-1449.
22. Strand, L. D., Nguyen, M. H., and Cohen, N. S., *Twenty-Fourth Joint Propulsion Conference*, 1988, AIAA Paper No. 88-3254.
23. Strand, L. D., and Cohen, N. S., *Twenty-Fifth Joint Propulsion Conference*, 1989. AIAA Paper No. 89-2528.
24. Strand, L. D., and Cohen, N. S., *JANAF Combustion Meeting*, 1990, CPIA Publication No. 557.
25. King, M. K., *J. Spacecraft and Rockets* 16:154–162 (1979).
26. King, M. K., *Eighteenth Symposium (International) on Combustion*, The Combustion Institute, Pittsburgh, 1981, pp. 207–216.
27. Williams, F. A., Barriere, M., and Huang, N. C., *Fundamental Aspects of Solid Propellant Rocket*, AGARD Report No. 116 1969.

28. Razdan, M. K., and Kuo, K. K., *AIAA J* 20:122–128 (1982).
29. Green, L. J., *Jet Propulsion* 24:9–15 (1954).
30. Kubota, N., *Eighteenth Symposium (International) on Combustion*, The Combustion Institute, Pittsburgh, 1981, pp. 187–194.
31. Paul, P. J., and Makunda, H. S., *Proceedings of the First National Conference on Air Breathing Engines and Aerospace Propulsion*, Interline Publishers, Bangalore, 1992, pp. 6–10.
32. Zucrow, M. J., Osborn, J. R., and Murphy, J. M., *AIAA J.* 3:523–525 (1965).

Received 31 March 1995